INTERNATIONAL JOURNAL OF HYDROGEN ENERGY 42 (2017) 6369–6383

Available online at www.sciencedirect.com

ScienceDirect

journal homepage: www.elsevier.com/locate/he

The effect of varying EGR and intake air boost on hydrogen-diesel co-combustion in CI engines

Midhat Talibi[*], *Paul Hellier*, *Nicos Ladommatos*

Department of Mechanical Engineering, University College London, Torrington Place, London WC1E 7JE, United Kingdom

ARTICLE INFO

Article history:
Received 20 September 2016
Received in revised form
12 November 2016
Accepted 25 November 2016
Available online 27 December 2016

Keywords:
Hydrogen
Co-combustion
Diesel engine
Intake air boost
EGR
Exhaust emissions

ABSTRACT

This paper presents a H_2-diesel fuel co-combustion study undertaken on a supercharged, direct injection, diesel engine investigating the combustion characteristics and emissions production at a range of engine loads (IMEP), EGR levels and intake air boosting conditions. The utilisation of EGR and intake air boost with H_2-diesel fuel co-combustion allows simultaneous NO_x and particulate emissions reduction at conditions closer to on-road driving conditions.

The results showed that while H_2 can be favourable in reducing CO_2 and particulate emissions, it causes an increase in NO_x emissions when the intake energy contribution from H_2 is increased. A reduction in the number of fine and ultrafine particles (diameter 0.05–0.2 μm) was observed when H_2 was added to the engine, especially at the low and intermediate intake air boost levels. At high EGR levels (equivalent to 2% intake O_2 concentration reduction) significant reductions in exhaust particulate mass of up to 75% were observed at 15% energy from H_2. An attempt was made to identify the optimum H_2 operating window at the different engine loads, intake air boost and EGR levels.

Introduction

Global demand for liquid fuels is projected to rise at a rapid pace – almost 37% – by 2040 [1]; however, current and future energy policies are increasingly aiming to reduce carbon emissions from the transport sector. The combustion of fossil fuels releases carbon, in the form of carbon dioxide (CO_2), and there is consensus that the rapid anthropogenic emission of fossil bound carbon is resulting in global climate change. Co-currently, there is growing awareness of the negative impacts of toxic exhaust pollutants from internal combustion engines, such as nitrogen oxides (NO_x) and carbonaceous soot or particulate matter (PM), on the health of urban populations.

The co-combustion of diesel fuel with gaseous fuels such as natural gas [2–5], biogas [6–12] and hydrogen [13–19] has been carried out in the past to reduce exhaust pollutant emissions. Natural gas is primarily composed of methane which has a lower carbon-to-hydrogen ratio compared to diesel fuel, and hence produces lower carbon emissions post combustion [20]. Biogas is considered to be a carbon-neutral fuel as it utilises carbon captured by plants during photosynthesis [21]. Biofuels derived from agricultural biomass offer the added advantage of reducing dependence on fossil liquid fuels [22–24]. Rajesh Kumar et al. [24] conducted tests with advanced biofuels and managed to achieve simultaneous NO_x-smoke reduction at certain operating conditions,

* *Corresponding author.*
E-mail addresses: m.talibi@ucl.ac.uk, midhattalibi@hotmail.com (M. Talibi).
http://dx.doi.org/10.1016/j.ijhydene.2016.11.207

however, an increase in HC and CO emissions was observed. Furthermore, gaseous fuels like natural gas and biogas have lower flame propagation speeds compared to diesel fuel, and therefore can result in reduced engine thermal efficiencies [9,25]. Hydrogen (H_2) has the potential to be an important energy carrier for the future for sustainable provision of power with reduced impact on the environment. H_2 has no carbon content and the co-combustion of H_2 and diesel fuel can potentially reduce levels of both exhaust gas CO_2 and PM. Hydrogen requires a very low amount of energy to ignite but has high flame propagation rates within the engine cylinder in comparison to hydrocarbon fuels, even at lean mixture conditions [26]. Therefore, the displacement of fossil diesel fuel with H_2 is an attractive proposition for compliance with emissions standards and reduction of harmful pollutants from diesel engines.

Several studies have been conducted in the past on co-combusting H_2 with diesel fuel in naturally aspirated CI engines [27–31]. While these investigations reported a decrease in carbon emissions (as a result of direct displacement of fossil diesel fuel by H_2) a significant increase in NO_x emissions was observed when the combined temperatures resulting from H_2-diesel fuel co-combustion exceeded the thermal NO_x formation temperatures [27]. The increased levels of NO_x emissions were considered to be due to higher peak flame temperatures of H_2, as compared to diesel fuel, which increased in-cylinder gas temperatures [14,28].

Exhaust gas recirculation (EGR) is a commonly employed NO_x reduction technique whereby exhaust gas is recirculated into the inlet manifold to mix with fresh intake air before entering the combustion chamber [32,33]. EGR reduces combustion gas temperatures, and hence decreases NO_x formation rates, either by diluting the fresh intake air (and effectively reducing the intake O_2 concentration) or due to an increased proportion of higher specific heat capacity components, such as CO_2, in the intake charge. Various researchers have successfully used EGR to minimize the high NO_x emissions produced as a consequence of H_2 combustion in diesel engines [17,34–36]. For example, Saravanan and Nagarajan. [17] aspirated H_2 in a single-cylinder, direct-injection diesel engine and used 15% and 25% EGR for NO_x reduction. The authors observed an increase in brake thermal efficiency of 1.35% when co-combusting H_2 and diesel fuel as compared to neat diesel operation, which was attributed to H_2 operating at leaner equivalence ratios than diesel fuel. The efficiency fell slightly (about 0.5%) with the introduction of EGR into the engine, as a result of dilution of the intake charge [17]. As expected, NO_x emissions increased when diesel was increasingly substituted with H_2, and considerably reduced when EGR was introduced – NO_x emissions decreased by almost 21% with 25% EGR. An almost 50% reduction in smoke was observed with H_2-diesel co-combustion, as compared to neat diesel operation, primarily due to substitution of carbon by hydrogen. However, an increase in smoke was reported with EGR, attributable to the reduction in the proportion of oxygen in the intake charge, and hence a decrease in carbon oxidation rates [17]. The authors concluded that the use of H_2 as a secondary fuel with diesel, combined with the use of EGR, can be a viable exhaust NO_x and PM emissions reduction strategy [17]. Bose and Maji [34]also conducted H_2-diesel dual fuel tests on a Kirloskar single cylinder CI engine and reported observations of NO_x, smoke and brake thermal efficiency very similar to those of Saravanan and Nagarajan [17]. Miyamoto et al. [35] attempted to reduce the trade-off between NO_x and smoke production in a diesel engine, operated with H_2 as a secondary fuel, by utilizing EGR for low temperature combustion (LTC). The authors varied the diesel fuel injection timing, volumetric proportion of H_2 in the intake charge and EGR rate and reported a specific set of engine operating conditions (2 CAD BTDC diesel injection, 3.9% H_2 v/v and 20% EGR) when the NO_x and smoke emissions were at acceptably low levels, cyclic variation was minimal and the indicated thermal efficiency had been reduced by approximately 1% as compared to neat diesel fuel, zero EGR operation [35]. Shin et al. [36] utilized cooled EGR in order to control NO_x emissions in a H_2 fuelled, common rail diesel engine in which a modified inlet manifold allowed the temperature of the intake charge to be maintained at 25 °C. The authors reported a slight improvement in brake thermal efficiency with increasing H_2, and significant reductions in NO_x emissions (25%) were observed at high EGR rates (31%). However, an increase in exhaust emissions of unburned hydrocarbons and carbon monoxide was also reported, attributable to the reduction in intake O_2 by both the aspirated H_2 and EGR [36]. More recently, Banerjee et al. [37] reviewed the synergy between hydrogen and EGR as a potential pathway to reduce both carbon and NO_x emissions. The study [37] commented that the use of H_2 allowed the prospect of applying heavy EGR to diesel engines and has the potential to achieve a trade-off between NOx-PM-BSFC, which would not be possible with conventional diesel combustion.

While the use of EGR with H_2-diesel co-combustion has been shown to reduce exhaust NO_x emissions, several studies covered in the above literature survey, also demonstrate that the displacement of intake O_2 by both H_2 and EGR causes an increase in exhaust smoke, unburned hydrocarbons and soot emissions. Intake air pressure boosting is an effective technique which allows a greater amount of O_2 to be supplied to the combustion chamber by increasing the density of the intake charge, thereby enhancing the maximum power output from an engine [38–40]. Nagalingam et al. [41], Furuhama and Fukuma [42] and Lynch [43] carried out some of the early investigations on boosted H_2-fuelled engines. Nagalingam et al. [41] reported NO_x levels below 100 ppm when operating at a supercharged intake pressure of 2.6 bar. More recently, Roy et al. [44] investigated the combustion and emission characteristics of a supercharged engine, fuelled by H_2 and pilot ignited by diesel fuel. The authors managed to attain almost 90% H_2 energy substitution with the engine operating at a brake thermal efficiency of 42% and almost zero smoke, CO (5 ppm) and HC (15 ppm) exhaust emissions [44]. Charge dilution was then performed by using N_2 gas which lowered NO_x emissions to almost negligible levels, and also allowed a higher amount of energy to be supplied from H_2 without H_2 autoignition prior to diesel pilot ignition [44].

The above work by Roy et al. [44] demonstrates that the utilisation of intake air boosting along with EGR could be an effective strategy in controlling exhaust emissions, particularly NO_x and smoke, in a H_2 fuelled diesel engine, especially when operating at high engine loads. However literature on

this subject is still limited, especially when determining the effect of intake air boosting and EGR, in conjunction with H_2-diesel fuel co-combustion, on exhaust particulates. The current study investigates the effects of increasing the percentage of energy supplied to the engine from H_2 (while reducing that from diesel fuel) on combustion characteristics and emissions production at a range of engine loads (IMEP), EGR levels and intake air boosting combinations. N_2 gas was used to dilute the intake charge and reduce the intake O_2 concentration in order to simulate EGR-like conditions inside the combustion chamber. The work also focuses on the effect of H_2 concentration, EGR and intake air boosting on exhaust particulate size and number distribution. The last part of the paper attempts to find an optimum H_2 operating window based on the exhaust emission results.

Experimental setup

The study described in this paper was carried out on a 4 stroke, water-cooled, common rail diesel engine, described in detail in a previous publication [27]. A 2.0 litre, 4-cylinder Ford Duratorq cylinder head was mounted on a Ricardo Hydra crankcase to form a single-cylinder research engine. The engine in-cylinder gas pressure was measured every 0.2 CAD using the Kistler 6056A piezoelectric transducer, which was being pegged every engine cycle to the inlet manifold pressure at the piston BDC position. The in-cylinder pressure, along with other pressure and temperature measurements were logged in to PCs using National Instruments data acquisition systems. A servo-hydraulic solenoid valve injector was used for diesel fuel injection, with the fuel injection pressure, injection timings and duration being controlled by the Emtronix EC-GEN 500 system. H_2 gas was supplied from a compressed gas bottle, via a mass flow controller (Bronkhorst F-201AV-70K, accuracy ±0.08 l/min) and fed into the engine inlet manifold 350 mm upstream of the intake valves. EGR-like conditions were simulated in the engine test rig by aspirating N_2 gas with the intake air to reduce the O_2 concentration entering the engine cylinder. The flow of N_2 into the intake manifold was also controlled using a Bronkhorst mass flow controller (F-202AV-70K), with an accuracy of ±0.15%.

Exhaust gas measurements of CO, CO_2, THC, NO_x and O_2 concentrations were performed using a Horiba MEXA-9100HEGR automotive gas analyser rack. The analyser rack houses a non-dispersive infrared absorption analyser for CO (±1 ppm) and CO_2 (±0.01%) emissions, a chemiluminescence analyser for NO_x (±1 ppm) measurements, a flame ionization detector for THC emissions (±10 ppm) and a magneto-pneumatic analyser to measure oxygen (±0.1%) concentrations. The exhaust particulate number and size distribution were measured using the Cambustion DMS500 differential mobility spectrometer. Exhaust gas samples were taken 30 cm downstream of the exhaust valves and conveyed to the analysers via heated lines, which were maintained at 190 °C and 80 °C for the measurement of gaseous and particulate compositions respectively.

An intake air supercharger system was deployed on the research engine to create test conditions that match a modern turbocharged engine, while allowing for independent control of intake air pressure and temperature. The system contained a rotary screw supercharger (Eaton M45), driven by an ABB electric motor via a drive belt. The speed of the electric motor was controlled by a thyristor system with a voltage of 0–10 V adjusted by means of a potentiometer. A Bowman charge-air cooler was mounted downstream of the supercharger to control the temperature of air entering the intake manifold, and a positive displacement volumetric air-flow metre (Romet G65), mounted upstream of the supercharger, was used to determine the air flow rate. The level of intake air boosting was determined by measuring the inlet manifold pressure, using a Druck piezoresistive transducer installed 160 mm upstream of the inlet valves. Fig. 1 shows a schematic of the test facility, while Table 1 lists the geometrical specifications and other particulars of the engine setup.

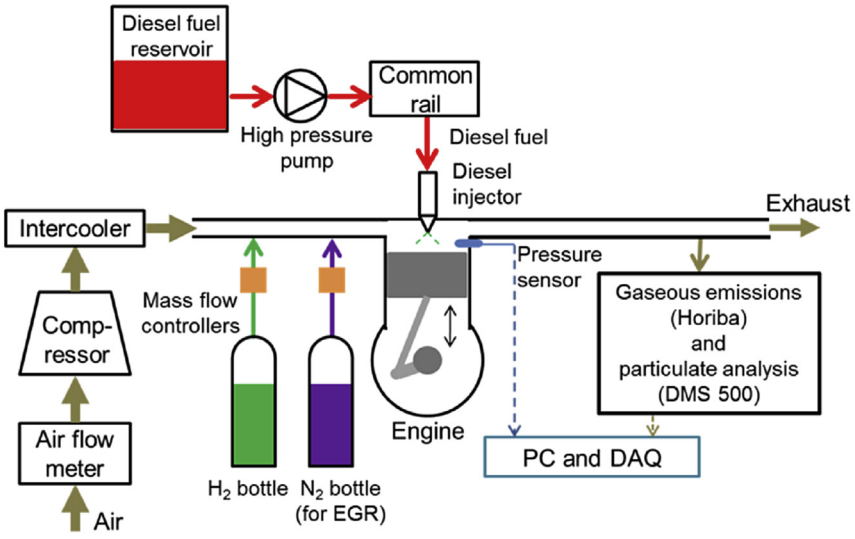

Fig. 1 – Schematic of the test facility including the supercharger setup and exhaust analysis systems.

Table 1 – Engine specifications.

Bore	86 mm
Stroke	86 mm
Swept volume	499.56 cm^3
Compression ratio (geometric)	18.3: 1
Maximum in-cylinder pressure	150 bar
Piston design	Central ω – bowl in piston
Fuel injection pump	Delphi single-cam radial-piston pump
High pressure common rail	Delphi solenoid controlled, 1600 bar max.
Diesel fuel injector	Delphi DFI 1.3 6-hole solenoid valve
Electronic fuel injection system	1 μs duration control
Crank shaft encoder	1800 ppr, 0.2 CAD resolution
Oil and coolant temperature	80 ± 2.5 °C

Experimental methodology

For all the experiments conducted in this work, the engine speed was fixed at 1200 rpm, and diesel fuel was injected at a common rail pressure of 900 bar and at constant diesel fuel injection of 6 CAD BTDC. The fuel injection timing of 6 CAD BTDC was optimised for the diesel only tests. The diesel fuel used was of fossil origin with zero fatty acid methyl ester (FAME) content, cetane number of 53.2 and carbon to hydrogen mass ratio of 6.32:1. Compressed H_2 gas of purity 99.995% and compressed N_2 gas of purity 99.5% were obtained from a commercial gas supplier (BOC). All the tests were repeated at a higher engine speed of 2200 rpm and similar trends in combustion and exhaust emission characteristics were obtained. In order to avoid repetition, these results have not been included in this paper.

Table 2 shows the test conditions used for the combined EGR and intake air boost tests. For each engine load (IMEP) the amount of H_2 and diesel fuel, supplied to maintain a constant engine load, were varied to change the energy contribution of H_2 as a function of the total energy supplied to the engine. The 'diesel only' test points were repeated several times in order to monitor engine drift and the following COV values of exhaust emissions for diesel only repeat tests were obtained: COV (CO_2) – 0.0087; COV (THC) – 0.1357; COV (NO_x) – 0.0122; COV (TPM) – 0.0394. The measured volumetric flow rates of N_2 gas and intake air were used to calculate the amount of O_2 reduction (v/v) in the intake air due to the aspirated N_2 gas, while the pressure transducer and thermocouple mounted in the engine intake manifold monitored the intake boost pressure and temperature, respectively. It should also be noted here that when both H_2 and N_2 were being aspirated into the engine, the flowrates of both gases were adjusted so as to keep the reduction in intake O_2 constant. For example, when the percentage energy from H_2 was increased (by increasing the H_2 flow rate), the flow rate of N_2 was decreased, so as to keep the intake O_2 reduction constant. Table 2 also shows the corresponding engine power output for each load (IMEP); in each instance this corresponds to the half-litre single cylinder engine used for all tests, and has not been scaled to represent an equivalent two litre, four cylinder engine. Table 3 shows the density and lower heating values of the diesel fuel and H_2 gas utilised in these experiments [14]. Fig. 2 shows the energy supplied to the single-cylinder research engine from H_2 as a function of the total energy supplied to the engine (energy supplied from H_2 plus the energy supplied from diesel fuel); the corresponding H_2 flow rates and the power content of H_2 supplied to the engine are also shown in Fig. 2a and b, respectively.

Some preliminary tests were conducted to determine the combustion efficiency of H_2 through measurement of unburned H_2 levels in the exhaust. The level of H_2 in the exhaust was considered to be the H_2 remaining unburned during combustion, as diatomic hydrogen is unlikely to have formed from diesel hydrogen content. The exhaust gas composition was analysed for H_2 at different engine loads using a gas chromatograph system with a thermal conductivity detector (GC-TCD), and measurements of the H_2 exhaust levels at varying loads corresponded to an average value of 10% of the H_2 supplied to the engine remaining unburned. This value is in good agreement with previous measurements under similar diesel fuel co-combustion operating conditions by Christodoulou & Megaritis [15]. In addition, a smaller amount of aspirated H_2 is expected to have been lost due to blow-by past the piston rings during the compression and early combustion stages.

Table 2 – Test operating condition matrix showing different intake air boost-engine load combinations at various EGR ratios and engine speed 1200 rpm.

Intake air boost pressure (bar)	Intake temperature (°C)	Engine load (bar IMEP)	Indicated engine power (kW)	% points O_2 reduction (v/v)
1.33	30	8.5	4.25	Only H_2 (no N_2)
				1
				2
				3
1.67	30	10	5.00	Only H_2 (no N_2)
				1
				2
				3
1.99	30	11.5	5.75	Only H_2 (no N_2)
				1
				2
				3

Results and discussion

Combustion characteristics

Fig. 3 shows the in-cylinder gas pressure and apparent net heat release curves for two intake air boost-engine load combinations, for 15% and 28% energy contribution from H_2 of

Table 3 – Densities and lower heating values of diesel fuel and hydrogen at 1 atm and 300 K [8].

Property	Diesel fuel	Hydrogen
Density (kg/m^3)	831.9	0.0838
Lower heating value (MJ/kg)	43.14	120

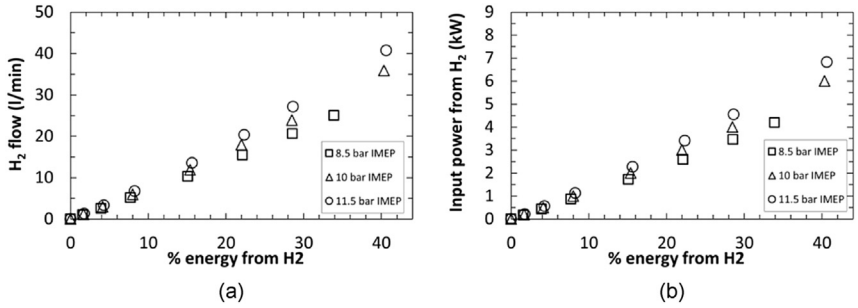

Fig. 2 – H_2 flow rates (l/min) and (b) power content of H_2 (kW) at constant engine loads and varying percentage energy from H_2.

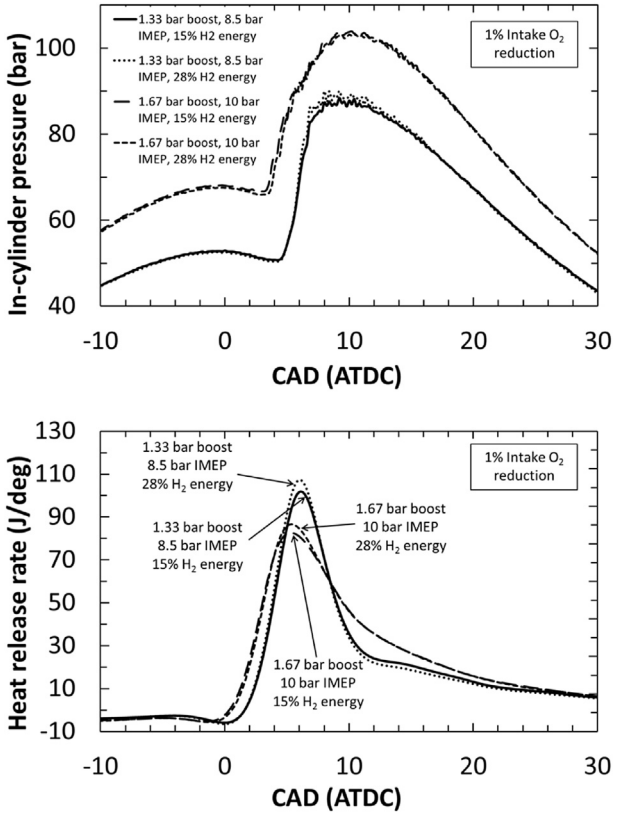

Fig. 3 – (a) In-cylinder gas pressure and (b) apparent net heat release rate curves at constant intake air pressure – engine load combinations and varying % energy from H_2 at an intake O_2 reduction level of 1%.

the total energy (from H_2 plus diesel fuel) supplied to the engine. The in-cylinder pressure traces shown are an average of 250 consecutive engine cycles for that particular test point. The in-cylinder pressure data was utilised to evaluate the net apparent heat release rates and the indicated mean effective pressure (IMEP), utilizing a one dimensional and single zone thermodynamic model and assuming homogenous conditions and ideal gas behaviour [38]. For all the heat release curves shown in Fig. 3, the reduction in intake O_2, by aspirating N_2 to simulate EGR-like conditions in the cylinder, is 1%. For both the intake air boost-engine load conditions, it can be observed that increasing the energy contribution from H_2 increases the peak heat release rates, but does not have a significant effect on the duration of ignition delay. It is also interesting to note that while for the 1.33 bar intake air pressure the premixed combustion stage and diffusion burning stage can be clearly distinguished, the 1.67 bar boost heat release curves appear as one long premixed stage. This could be due to the higher levels of turbulence created inside the cylinder at the higher boost condition, leading to enhanced fuel-air mixing rates. The differences in duration of ignition delay and peak heat release rates are discussed in more detail in the following paragraphs.

Fig. 4 shows the duration of ignition delay for three intake air boost pressure-engine load combinations, at constant percentage reductions in intake O_2 and varying percentage energy from H_2. The duration of ignition delay is defined as the time in crank angle degrees (CAD) between the start of the injection signal supplied to the diesel fuel injector (SOI) and the start of combustion (SOC) as indicated by the first incidence of positive heat release. Fig. 4 shows that an increase in intake air pressure leads to a decrease in the duration of ignition delay. This is likely to be the result of the increasing O_2 concentration accelerating the low temperature fuel oxidation rate during the ignition delay period. Additionally, higher intake air pressures result in higher effective compression ratios which, due to an increase in in-cylinder pressures and temperatures, also reduce the ignition delay. It can also be seen from Fig. 4 that for each intake air pressure, increasing the percentage reduction in intake O_2 (that is, decreasing the amount aspirated O_2) increases the duration of ignition delay. This could be attributed to the displacement of intake air O_2 with the aspirated N_2, which reduces the pool of reactive species available for combustion and thus the rates of low temperature diesel fuel breakdown and oxidation reactions, thus delaying SOC. Fig. 4 also shows that the substitution of diesel fuel with H_2 has little or no effect on the duration of ignition delay. However, it should be noted that since the resolution of the engine crankshaft encoder is 0.2 CAD, any changes in the ignition delay duration within this range can be a result of equipment variability and resolution errors. While no significant change in ignition delay with increasing H_2 was observed in this study, variations in ignition delay in previous literature have been explained due to the intake charge effective heat capacity and temperature, chemical kinetic processes (especially those occurring pre-diesel ignition) and oxygen concentration of the intake charge [45,46].

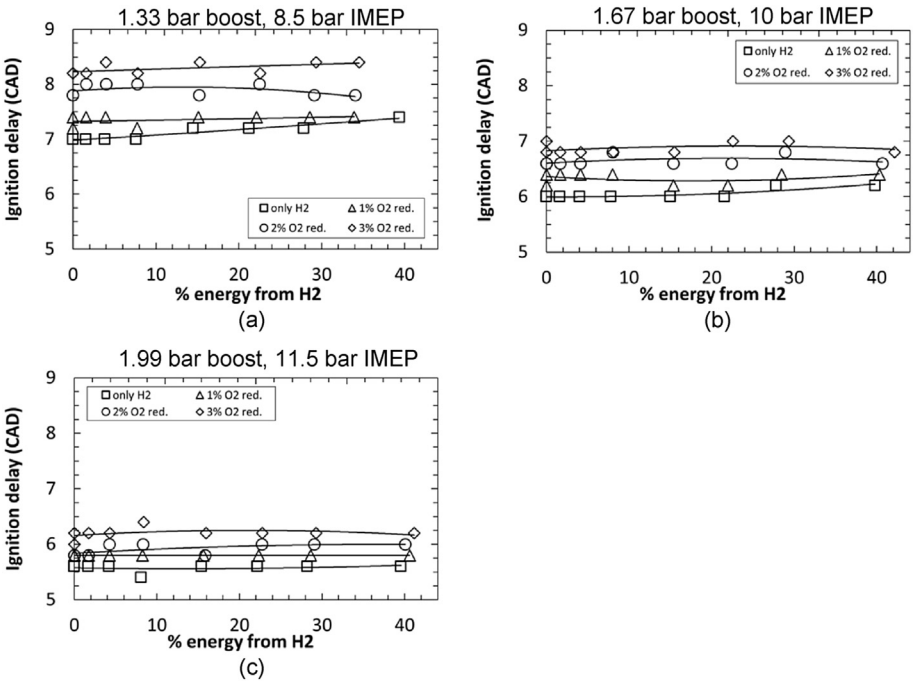

Fig. 4 – Duration of ignition delay for three intake air boost-engine load combinations, at constant percentage reductions in intake O_2 and varying percentage energy from H_2.

Fig. 5 shows the apparent net peak heat release rates (pHRR) for the three intake air boost pressure-engine load combinations, at constant percentage reductions in intake O_2 and varying percentage energy from H_2. It can be seen from Fig. 5 that an increase in the intake air pressure leads to a reduction in the magnitude of pHRR. This can be attributed to the shorter duration of ignition delay with increasing intake air pressure (as can be observed in Fig. 4), leading to less significant premixed burn stage and lower pHRRs. Fig. 5 also shows that at 1.33 bar and 1.67 bar intake air pressures, increasing the percentage reduction in intake O_2 (that is, decreasing the amount aspirated O_2) results in an increase in the magnitude of pHRR. This is due to an increase in the duration of ignition delay, as observed in Fig. 4a and b, which allows more time for the fuel and air to mix, resulting in a greater amount of premixed diesel fuel-air mixture, of appropriate stoichiometry, available to undergo combustion at SOC. Similarly, Fig. 5a and b shows an increase in the pHRR as the percentage energy from H_2 is increased. This is expected, as H_2 combusts in a premixed mode providing additional energy to that of the diesel fuel and, furthermore, H_2 burns at higher adiabatic flame temperatures compared to diesel fuel, leading to higher in-cylinder gas temperatures during combustion. Increasing the amount of H_2 being supplied to the engine promotes premixed H_2 combustion, resulting in higher peak HRRs. For very lean H_2-air mixtures, the low pHRR could be due to the considerably low H_2 flame speeds inside the combustion chamber. However, Fig. 5c shows no significant effect of either percentage O_2 reduction or H_2 substitution (up to 30% energy from H_2) on the magnitude of pHRR. This can likely be attributed to two factors: firstly, the change in the duration of ignition delay due to increasing EGR is relatively small, secondly, the air flow rate at intake air pressure of 1.99 bar is quite high (approx. 980 l/min), which means that even at the highest percentage energy input from H_2 of 41%, the H_2 flow rate is relatively low (40 l/min) resulting in a very lean H_2-air mixture inside the combustion chamber, and therefore lower flame temperatures during combustion.

Exhaust gas emissions

Fig. 6 shows the specific exhaust gas emissions of carbon dioxide (CO_2) for the three intake air boost pressure-engine load combinations, at constant percentage reductions in intake O_2 and varying percentage energy from H_2. It can be seen from Fig. 6 that at all the three intake air pressure-load combinations, a decrease in the specific emissions of CO_2 is observed as diesel fuel is substituted by H_2 (increase in percentage energy from H_2). This is expected as carbon containing diesel fuel is replaced by H_2 which does not produce CO_2 as a combustion product.

Fig. 7 shows the specific exhaust gas emissions of unburned total hydrocarbons (THC) for the three intake air boost pressure-engine load combinations, at constant percentage reductions in intake O_2 and varying percentage energy from H_2. It can be seen from Fig. 7 that at all the three intake air boost pressure-engine load combinations, decreasing the intake O_2 concentration to 1% results in a decrease in THC emissions, with any further decrease in intake O_2 leading to an increase in THC emissions. The initial decrease in THC emissions may be due to an increase in the duration of ignition delay (as was observed in Fig. 4), allowing more time for diesel fuel and air to mix prior to SOC. Further reduction in intake O_2 concentration above 1% may severely affect the availability of O_2 for diesel fuel oxidation, prevailing over the

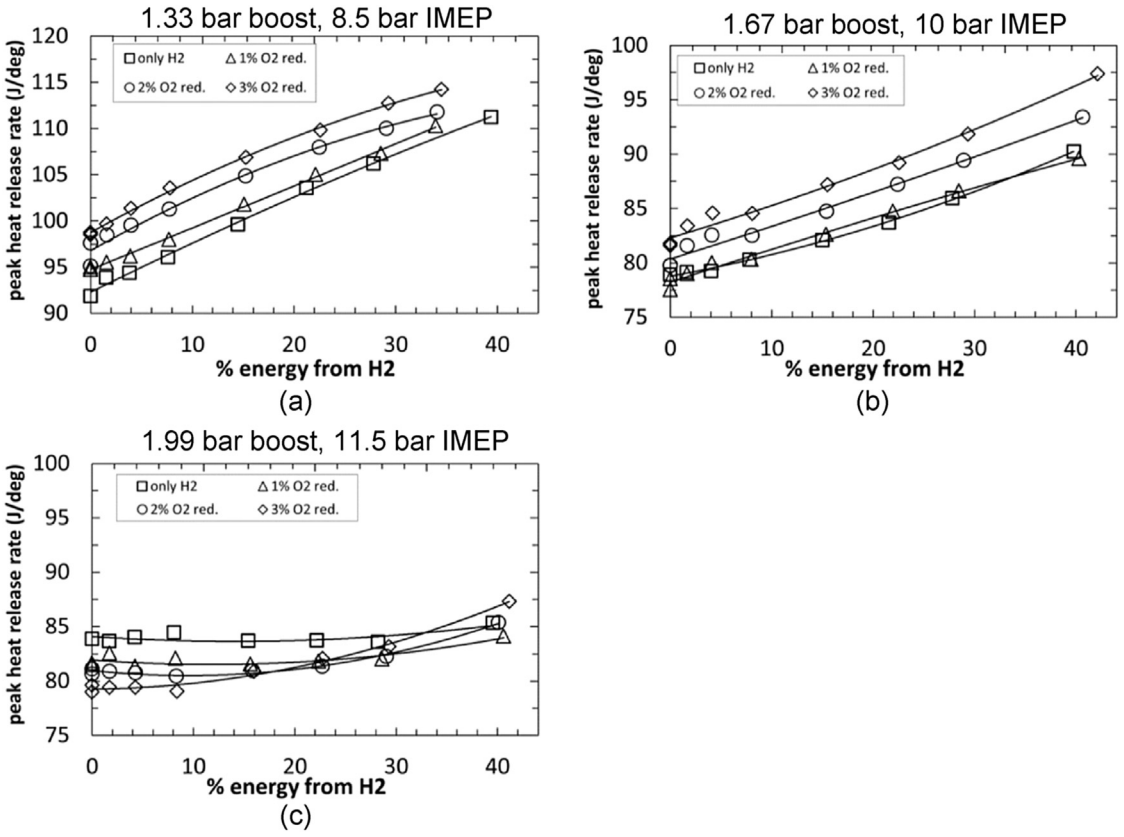

Fig. 5 – Peak heat release rates (J/deg) for three intake air boost-engine load combinations, at constant percentage reductions in intake O_2 and varying percentage energy from H_2.

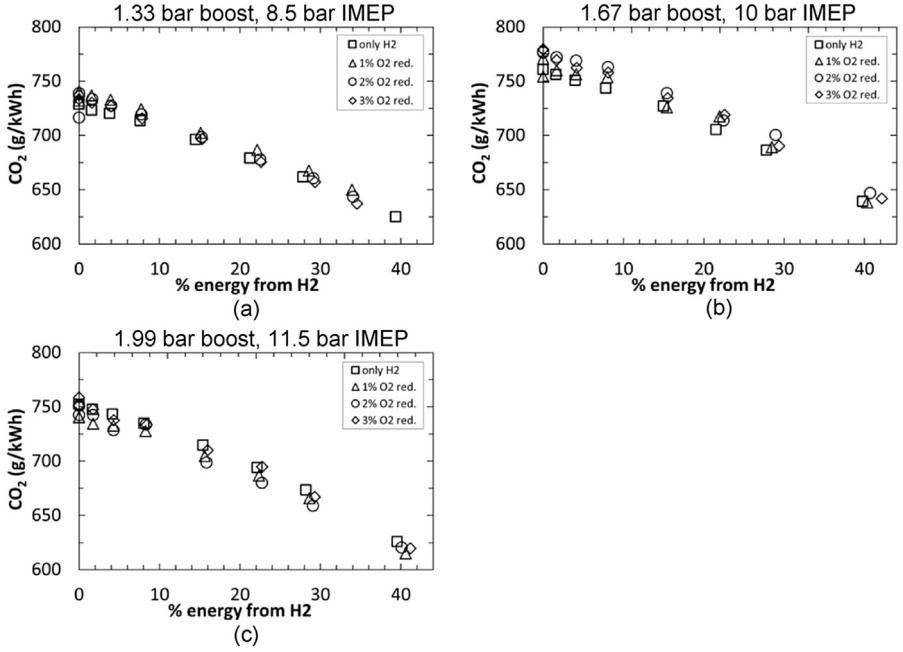

Fig. 6 – Specific emissions of carbon dioxide (CO_2) for three intake air boost-engine load combinations, at constant percentage reductions in intake O_2 and varying percentage energy from H_2.

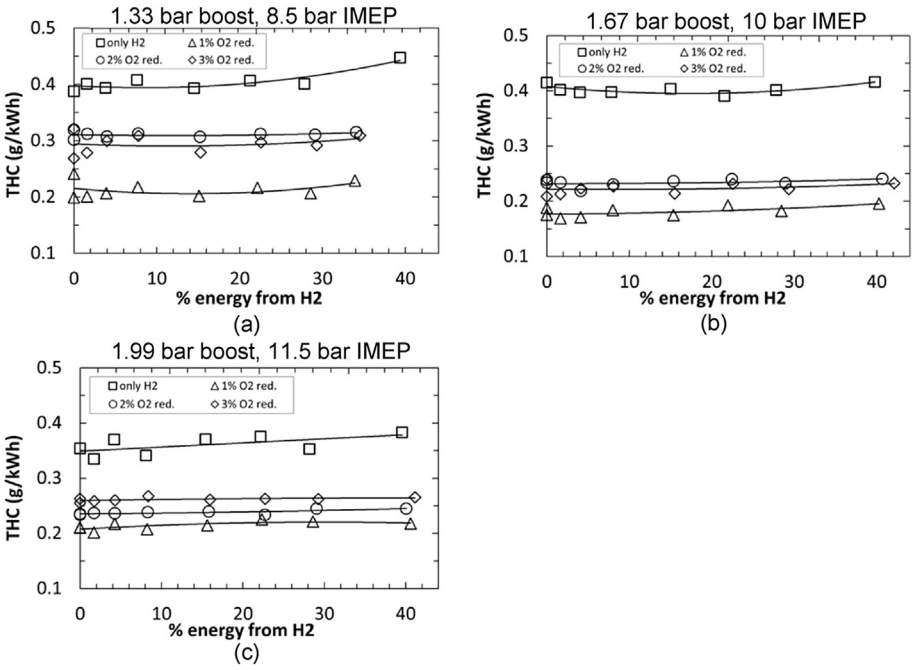

Fig. 7 – Specific emissions of unburned total hydrocarbons (THC) for three intake air boost-engine load combinations, at constant percentage reductions in intake O_2 and varying percentage energy from H_2.

influence of increased ignition delay on combustion phasing, and lead to increased THC emissions. Fig. 7 does not show an apparent effect of displacement of diesel fuel by H_2 on THC emissions. This might be because, at such relatively high engine loads of 8.5 bar IMEP and above, a substantial quantity of diesel fuel (diesel fuel flow rate ≈ 18 ml/min) is being injected in the combustion chamber and the displacement of some of this diesel fuel by H_2 is not sufficient to have a significant effect on unburned THC exhaust emissions.

Fig. 8 shows the specific exhaust gas emissions of oxides of nitrogen (NO_x) for the three intake air boost pressure-engine load combinations, at constant percentage reductions in intake O_2 and varying percentage energy from H_2. The effect of reducing intake O_2 on exhaust NO_x emissions is very apparent from Fig. 8, for example, at 1.67 bar intake air pressure and 8% energy from H_2, a 67% decrease in NO_x emissions is observed when intake O_2 level is reduced by 1%. This is expected, as the aspirated N_2 displaces the intake O_2 which is required for fuel oxidation and for thermal oxidation of N_2 to form NO_x, thereby lowering post combustion gas temperatures and reducing rates of NO_x formation.

A slight decrease in NO_x emissions is observed at low levels of H_2 substitution (<5–10% energy from H_2) at all three intake air boost pressures in Fig. 8. However, any further displacement of diesel fuel results in an increase in exhaust NO_x levels. This can be explained by the following: Diesel fuel injected into the combustion chamber of a diesel engine can always be expected to produce significant quantities of NO_x because combustion of the spray takes place around the spray fringe where the diesel fuel-air equivalence ratio is at an approximately stoichiometric value. As diesel fuel is progressively removed and replaced by H_2, this high rate of NO_x production from diesel fuel is curtailed. At the same time NO_x production from H_2 is not significant, because at such low levels of the H_2 substitution, the H_2-air equivalence ratio is still not sufficiently high for commensurate NO_x production (or production at the same levels produced by the diesel fuel for which the H_2 had been substituted). Hence a small drop in exhaust NO_x emissions is observed. As the amount of H_2 is increased, it appears that H_2 enhances the production of NO_x by further raising the temperatures in the diesel fuel spray combustion zones. Therefore, it seems that the H_2 provides, locally, additional synergetic heat release and temperature rise, resulting in extra NO_x formation, above NO_x emission levels due to diesel fuel alone at a constant EGR level. This phenomenon was also observed when co-combusting H_2 and diesel fuel in a naturally aspirated engine [27].

Fig. 9 shows the specific exhaust gas emissions of total particulate mass (TPM) for three intake air boost pressure-engine load combinations, at constant percentage reductions in intake O_2 and varying percentage energy from H_2. Fig. 9 shows that at 0% energy from H_2 (that is, with only diesel fuel and no H_2 substitution), a substantial increase in exhaust TPM levels is seen when the reduction in intake O_2 concentration is greater than 1%. This is a similar trend to that observed for exhaust THC emissions (Fig. 7), and is due to the reduction in O_2 availability as a result of displacement of intake air by N_2, resulting in reduced oxidation of soot precursors in the diesel fuel spray and soot particles already formed. The decrease in TPM levels as the percentage energy from H_2 is increased is a result of replacing diesel fuel with a zero-carbon fuel (H_2). The decrease in TPM levels is most apparent for the highest level of percentage O_2 reduction of 3% at all three intake air boost pressure-engine load combinations, for example at 1.99 bar intake air pressure and 3% intake O_2 reduction, a 50% drop in TPM level is observed at 15%

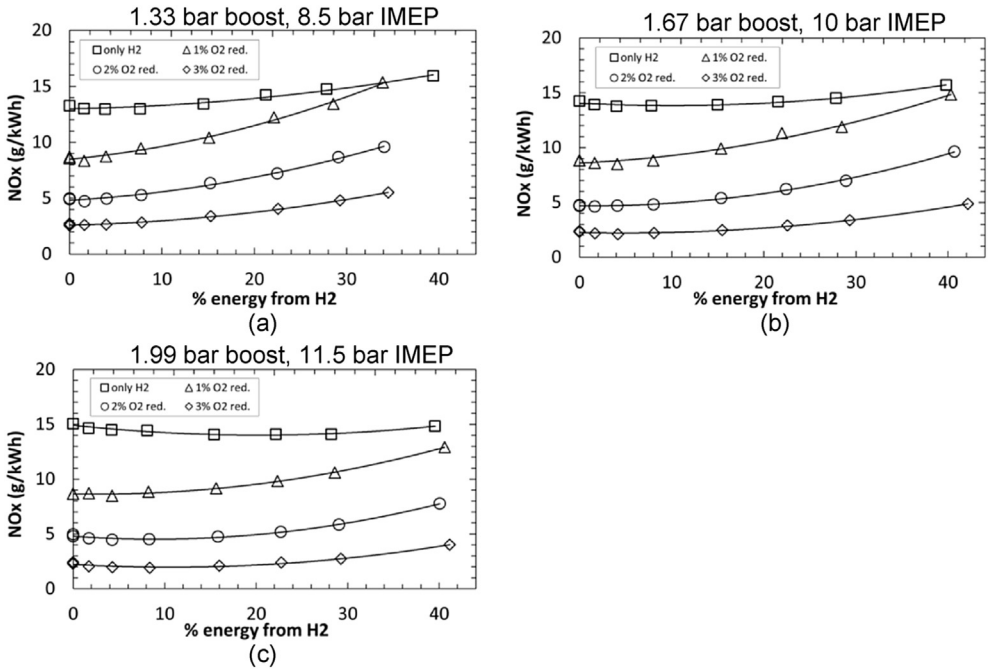

Fig. 8 – Specific emissions of oxides of nitrogen (NO_x) for three intake air boost-engine load combinations, at constant percentage reductions in intake O_2 and varying percentage energy from H_2.

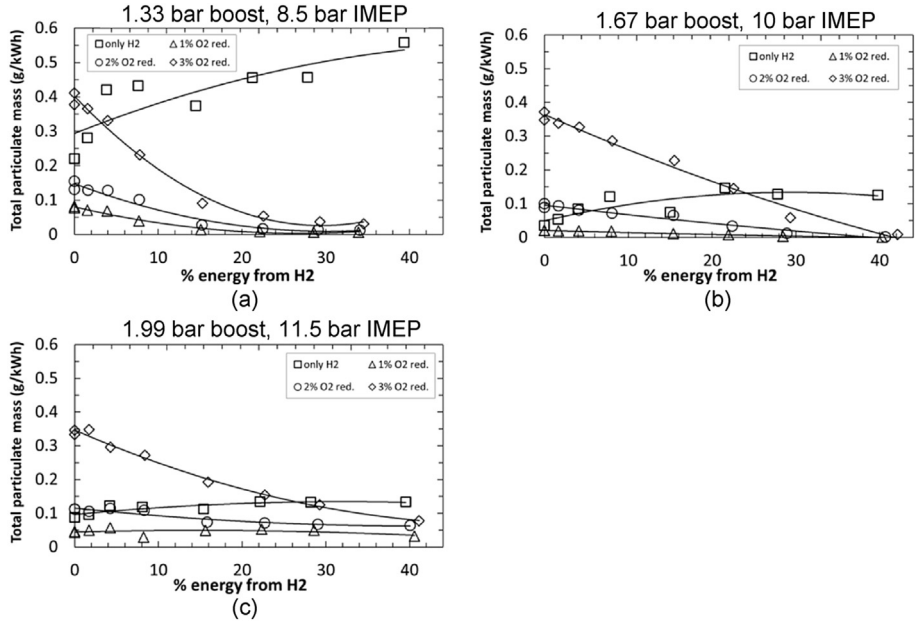

Fig. 9 – Specific emissions of total particulate mass for three intake air boost-engine load combinations, at constant percentage reductions in intake O_2 and varying percentage energy from H_2.

energy from H_2. Significant decreases in TPM levels of similar magnitude also occur at other percentage O_2 reduction levels, for example, at 1.33 bar intake air pressure and 2% intake O_2 reduction, a 75% drop in TPM level is observed at 15% energy from H_2. However, at the 1.33 bar intake air pressure condition and no EGR (that is, only H_2), an increase in TPM is observed when the percentage energy from H_2 increases from 0% to 5%. Further increase in H_2 energy up to 30% does not result in a significant change in TPM, but beyond 30% the TPM level again increases. Barring the increase in TPM at low % H_2 energy levels, the increase in TPM at high H_2 levels can be attributed to an effective reduction in intake O_2 due displacement by the aspirated H_2 [17,35,36].

Fig. 10a–c shows the size distribution of the number of particulates in the engine exhaust gas from tests conducted in this study for the three intake air pressure-engine load combinations, respectively, with various percentage reduction in intake O_2 and varying percentage energy from H_2.

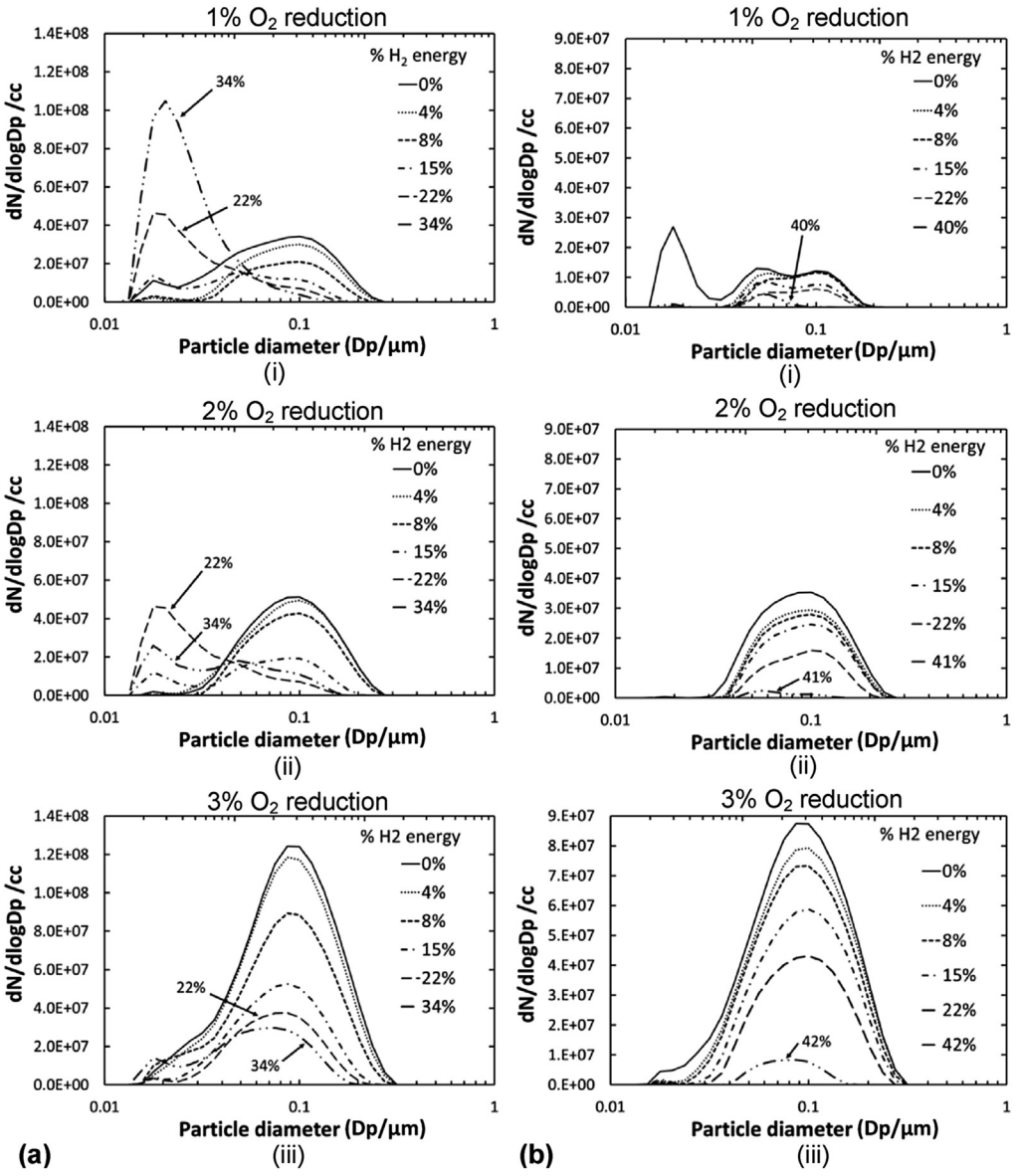

Fig. 10 – Particulate number distribution for (a) 1.33 bar intake air pressure – 8.5 bar IMEP engine load, (b) 1.67 bar intake air pressure – 10 bar IMEP engine load, at various percentage reduction in intake O_2 and varying percentage energy from H_2 and (c): Particulate number distribution for 1.99 bar intake air pressure – 11.5 bar IMEP engine load, at various percentage reduction in intake O_2 and varying percentage energy from H_2.

Fig. 11 shows a typical size distribution of diesel engine exhaust particles, both in terms of number of particles and total mass of particles, where particles have been divided into categories based on their diameters [47]. It can be seen from Fig. 11 that the bulk of the diesel engine particulates have diameters significantly lower than 1 μm and represent a mix of fine (Dp < 2.5 μm, PM2.5), ultrafine (Dp < 0.1 μm) and nanoparticles.

First, considering the effect of decreasing the amount of intake O_2 on the size distribution of the number of particulates, it can be seen from both Fig. 10a and b that as the O_2 level is decreased, the number of particles tends to increase significantly across the entire range of diameters (0.05–0.2 μm). As discussed previously (Fig. 9), this increase in the number of particles is due to the increasingly severe unavailability of O_2 (as it is displaced in the intake by the N_2) for diesel fuel combustion, which results in reduced rates of soot oxidation. The effect of decreasing the amount of intake O_2 on the particle distribution is not as evident at the highest intake boost-engine load combination of 1.99 bar boost-11.5 bar IMEP (Fig. 10c), apart from an increase in the number of particles of diameters ranging between 0.1 μm and 0.2 μm at the 3% O_2 reduction level. Since these particles are on the large end of the particle size spectrum, they account for most of the total particulate mass despite being fewer in number. This is the reason for the significant increase in total particulate mass emissions observed in Fig. 9c when the O_2 reduction level is increased to 3%.

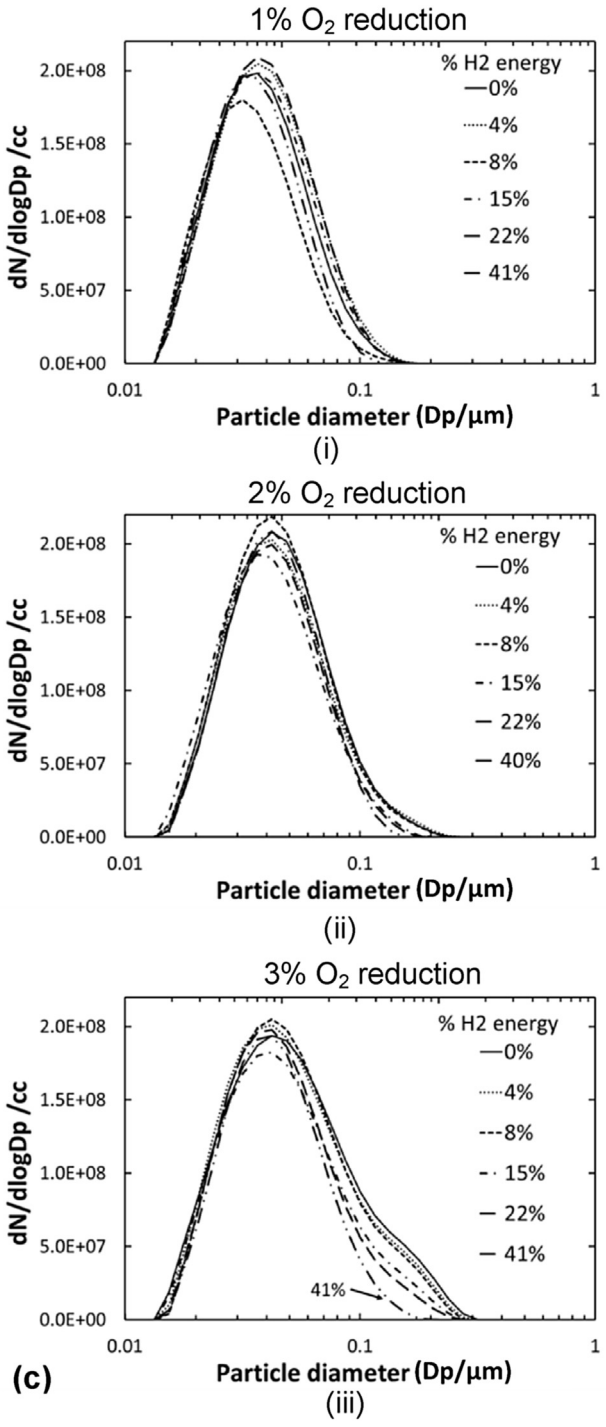

Fig. 10 – (*continued*)

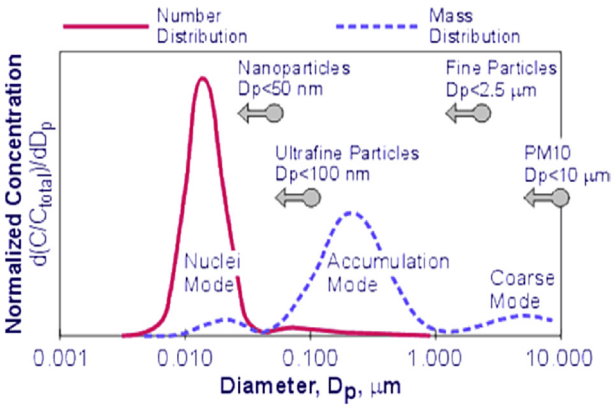

Fig. 11 – Typical size distribution of diesel exhaust particulates [47].

Now, considering the effect of H_2 at each percentage O_2 reduction level, it can be observed from Fig. 10a and b that the number of particles reduces as the percentage energy from H_2 is increased. The reduction primarily occurs for particles of diameters ranging between 0.05 μm and 0.2 μm which, as can be seen from Fig. 11, lie in the fine and ultrafine particle size range. The fine and ultrafine particles pose a serious health risk, as they can penetrate deeper into the lungs (as compared to particles in the PM10 size range) resulting in an increased risk of lung cancer, and cardiovascular and breathing disorders [48]. Hence, a reduction in the fine and ultrafine particles due to H_2 substitution could potentially be quite beneficial in diminishing the health hazards associated with particulates. As the percentage energy from H_2 is increased above 22% in Fig. 10a(i), a considerable increase in particulates of diameter lower than 0.02 μm is observed.

At the highest intake boost-engine load combination of 1.99 bar boost-11.5 bar IMEP (Fig. 10c), the effect of H_2 is not very distinct except at the 3% O_2 reduction level, where H_2 substitution results in the reduction of particles with diameters above 0.1 μm. As discussed before, since these large particles make up the majority of the total particulate mass, any reduction in the number of these large particles also results in a significant reduction in the total particulate mass (Fig. 9).

Indicated thermal efficiency

Fig. 12 shows the indicated thermal efficiency for the three intake air boost pressure-engine load combinations, at constant percentage reductions in intake O_2 and varying percentage energy from H_2. The amount of unburned H_2, not undergoing combustion and persisting to the exhaust, was taken into consideration when calculating the indicated thermal efficiency (following the preliminary exhaust H_2 measurement tests). It should be noted that in order to pressurise the intake air a supercharger was used which was, in effect, partially driving the engine. Additionally, in normal diesel engines the presence of the turbocharger in the exhaust manifold creates a back pressure, which was not the chase in this research engine. Therefore, preliminary calculations have shown that the thermal efficiency values shown here are slightly higher – by about 1.5–2% at the highest engine load of 1.99 bar IMEP.

Considering Fig. 12a (1.33 bar boost, 8.5 bar IMEP), it can be observed, at all three intake O_2 reduction levels, that the thermal efficiency initially decreases and then increases as the percentage energy from H_2 is increased. The initial decrease can be attributed to a lean H_2-air mixture displacing diesel fuel (which burns near-stoichiometric); this lean H_2-air mixture has slow flame propagation speeds and hence results

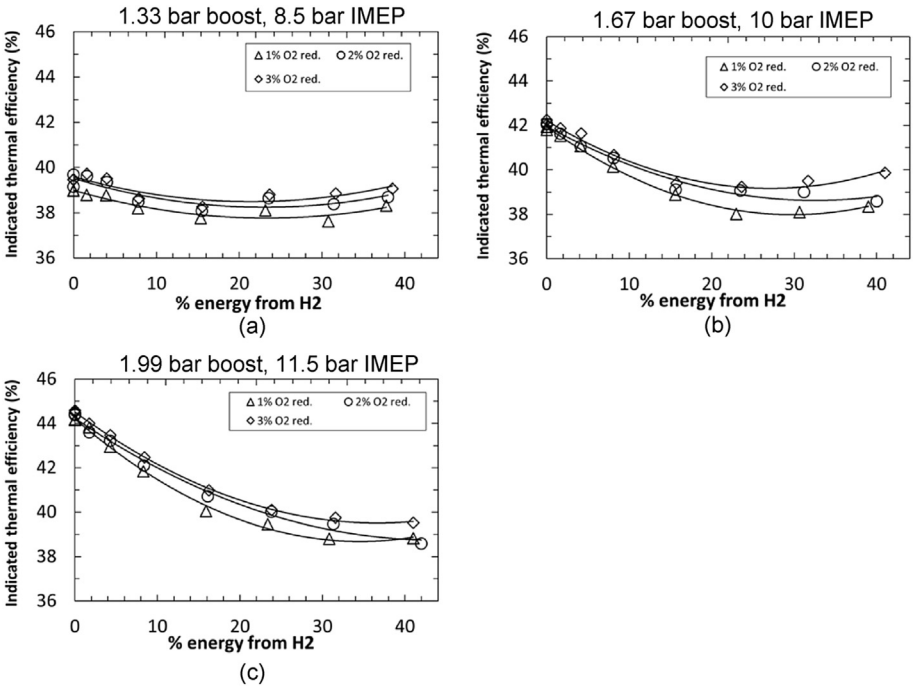

Fig. 12 – Duration of ignition delay for three intake air boost-engine load combinations, at constant percentage reductions in intake O_2 and varying percentage energy from H_2.

in a drop in thermal efficiency. As the mixture becomes less lean (at high H_2 substitution levels), the post-combustion in-cylinder temperatures increase resulting in an increase in thermal efficiency. Similar trends can also be observed at the other engine loads of 1.67 bar and 1.99 bar IMEP. Now considering the effect of increasing intake air boost pressure, it can be observed from Fig. 12 that thermal efficiency increases as the boost pressure is increased. This is expected, as increasing the boost pressure effectively increases the compression ratio inside the cylinder, resulting in higher pressures and temperatures at the end of the compression stroke.

Optimum H_2 operating window based on exhaust gas emissions results

Fig. 13a shows the specific emissions of NO_x and particulate mass for the three intake air boost pressure-engine load combinations, at a constant 1% intake O_2 reduction level and varying percentage energy from H_2. The 1% intake O_2 reduction level was chosen since the exhaust emission results demonstrated any further reductions in the intake O_2 concentration resulted in an increase in exhaust unburned hydrocarbon emissions, which is undesirable. It can be observed from Fig. 13a that NO_x exhaust emissions increase when the percentage energy from H_2 increases above 10%, however, below the 10% H_2 level NO_x emissions do not vary significantly. Therefore, based on Fig. 13a, it can be suggested that the use of H_2 would be favourable below a level of about 10% energy from H_2 (as shown inside the broken line rectangle on Fig. 13a), where there is no concurrent increase in NO_x emissions. Additionally, the greatest particulate reduction benefit

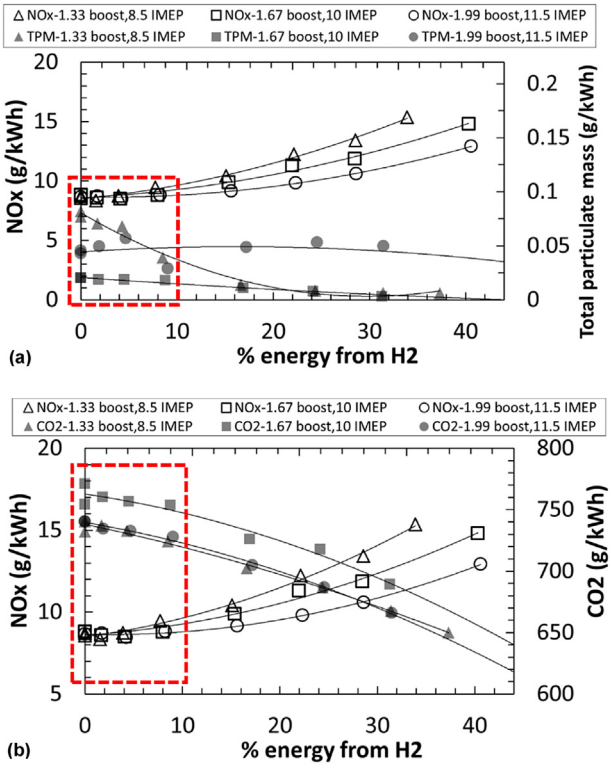

Fig. 13 – Specific emissions of (a) NO_x and total particulate mass and (b) NO_x and CO_2 for constant intake air pressure – engine load combinations and varying % energy from H_2, at an intake O_2 reduction level of 1%.

is obtained for the lowest intake air boost pressure-engine load combination (1.33 bar boost, 8.5 bar IMEP), where a 50% reduction in the specific emissions of total particulate mass can observed at the 10% H_2 energy contribution level (Fig. 13a). Similarly, Fig. 13b shows the benefit of H_2 in terms of CO_2 reduction whereby significant reductions in CO_2 can be obtained without an increase in NO_x emissions.

Conclusions

1. An increase in peak heat release rates was observed as the percentage energy being supplied to the engine from H_2 was increased. This was attributed to the extra heat release during H_2 premixed combustion and higher adiabatic flame temperatures of H_2 relative to diesel fuel.
2. Decreasing intake O_2 concentration by more than 1% resulted in an increase in the unburned hydrocarbon emissions due to O_2 unavailability for diesel fuel oxidation. No influence of H_2 on unburned hydrocarbon emissions was observed.
3. Specific emissions of NO_x were observed to increase but only when the energy contribution from H_2 was increased above the 10% level. This increase in NO_x emissions was attributed to H_2-diesel co-combustion resulting in higher in-cylinder temperatures relative to diesel fuel-only combustion.
4. Significant reductions in the total particulate mass were observed with increasing percentage energy from H_2 especially at high percentage O_2 reduction levels. For example, at the 1.33 bar intake air pressure – 8.5 bar IMEP engine load combination, and 2% intake O_2 reduction, a 75% drop in particulate mass is observed at 15% energy from H_2.
5. A reduction in the number of particles of diameter between 0.05 and 0.2 μm (in the range of fine and ultrafine particles) was observed with increasing percentage energy from H_2, specifically at the low (1.33 bar) and intermediate (1.67 bar) intake air boost levels.
6. Based on the exhaust emission results, it was suggested that H_2 can reduce CO_2 and particulate emissions with no concurrent increase in NO_x emissions when the energy contribution from H_2 is below the 10% level, at an EGR equivalent of 1% reduction in intake O_2 concentration for all the intake air boost pressures – engine loads combinations tested in this study.

Acknowledgements

The authors would like to acknowledge Cella Energy Ltd., Horiba MIRA Ltd. and Productive Group for support of this work, and Innovate UK (Project No. 101583) for their financial contribution to this project.

Nomenclature

ATDC	after-top-dead-centre
BTDC	before-top-dead-centre
CAD	crank angle degree
CI	compression ignition
CO	carbon monoxide
CO_2	carbon dioxide
EGR	exhaust gas recirculation
H_2	hydrogen
IMEP	indicated mean effective pressures
NO_x	nitrogen oxides
O_2	oxygen
PM	particulate mass
ppr	pulses per revolution
rpm	revolutions per minute
SOC	start of combustion
SOI	start of injection
TDC	top-dead-centre
THC	total hydrocarbons

REFERENCES

[1] Schiermeier Q. Energy outlook sees continuing dominance of fossil fuels. Nature News Blog. 2014. http://blogs.nature.com/news/2014/11/energy-outlook-sees-continuing-dominance-of-fossil-fuels.html [Accessed April 22 2015].
[2] McTaggart-Cowan GP, Rogak SN, Munshi SR, Hill PG, Bushe WK. Combustion in a heavy-duty direct-injection engine using hydrogen–methane blend fuels. Int J Engine Res 2009;10:1–13. http://dx.doi.org/10.1243/14680874JER02008.
[3] Gatts T, Liu S, Liew C, Ralston B, Bell C, Li H. An experimental investigation of incomplete combustion of gaseous fuels of a heavy-duty diesel engine supplemented with hydrogen and natural gas. Int J Hydrogen Energy 2012;37:7848–59. http://dx.doi.org/10.1016/j.ijhydene.2012.01.088.
[4] Imran S, Emberson DR, Ihracska B, Wen DS, Crookes RJ, Korakianitis T. Effect of pilot fuel quantity and type on performance and emissions of natural gas and hydrogen based combustion in a compression ignition engine. Int J Hydrogen Energy 2014;39:5163–75. http://dx.doi.org/10.1016/j.ijhydene.2013.12.108.
[5] Zhou JH, Cheung CS, Leung CW. Combustion, performance and emissions of a diesel engine with H_2, CH_4 and H_2–CH_4 addition. Int J Hydrogen Energy 2014;39:4611–21. http://dx.doi.org/10.1016/j.ijhydene.2013.12.194.
[6] Mohamed Ibrahim M, Varuna Narasimhan J, Ramesh A. Comparison of the predominantly premixed charge compression ignition and the dual fuel modes of operation with biogas and diesel as fuels. Energy 2015;89:990–1000. http://dx.doi.org/10.1016/j.energy.2015.06.033.
[7] Jung C, Park J, Song S. Performance and NOx emissions of a biogas-fueled turbocharged internal combustion engine. Energy 2015;86:186–95. http://dx.doi.org/10.1016/j.energy.2015.03.122.
[8] Bora BJ, Saha UK, Chatterjee S, Veer V. Effect of compression ratio on performance, combustion and emission characteristics of a dual fuel diesel engine run on raw biogas. Energy Convers Manag 2014;87:1000–9. http://dx.doi.org/10.1016/j.enconman.2014.07.080.
[9] Bari S. Effect of carbon dioxide on the performance of biogas/diesel duel-fuel engine. Renew Energy 1996;9:1007–10. http://dx.doi.org/10.1016/0960-1481(96)88450-3.
[10] Bedoya ID, Arrieta AA, Cadavid FJ. Effects of mixing system and pilot fuel quality on diesel-biogas dual fuel engine performance. Bioresour Technol 2009;100:6624–9. http://dx.doi.org/10.1016/j.biortech.2009.07.052.

[11] Barik D, Murugan S. Investigation on combustion performance and emission characteristics of a DI (direct injection) diesel engine fueled with biogas-diesel in dual fuel mode. Energy 2014;72:760–71. http://dx.doi.org/10.1016/j.energy.2014.05.106.
[12] Makareviciene V, Sendzikiene E, Pukalskas S, Rimkus A, Vegneris R. Performance and emission characteristics of biogas used in diesel engine operation. Energy Convers Manag 2013;75:224–33. http://dx.doi.org/10.1016/j.enconman.2013.06.012.
[13] Lambe S, Watson H. Optimizing the design of a hydrogen engine with pilot diesel fuel ignition. Int J Veh Des 1993;14:370–89.
[14] Saravanan N, Nagarajan G. Combustion analysis on a DI diesel engine with hydrogen in dual fuel mode. Fuel 2008;87:3591–9. http://dx.doi.org/10.1016/j.fuel.2008.07.011.
[15] Christodoulou F, Megaritis A. Experimental investigation of the effects of separate hydrogen and nitrogen addition on the emissions and combustion of a diesel engine. Int J Hydrogen Energy 2013;38:10126–40. http://dx.doi.org/10.1016/j.ijhydene.2013.05.173.
[16] Varde KS, Varde LK. Reduction of soot in diesel combustion with hydrogen and different H/C gaseous fuels. In: 5th World hydrogen energy, Toronto, Canada; 1984.
[17] Saravanan N, Nagarajan G. An experimental investigation of hydrogen-enriched air induction in a diesel engine system. Int J Hydrogen Energy 2008;33:1769–75. http://dx.doi.org/10.1016/j.ijhydene.2007.12.065.
[18] Hernández JJ, Lapuerta M, Barba J. Separate effect of H_2, CH_4 and CO on diesel engine performance and emissions under partial diesel fuel replacement. Fuel 2016;165:173–84. http://dx.doi.org/10.1016/j.fuel.2015.10.054.
[19] Mustafi NN, Raine RR, Verhelst S. Combustion and emissions characteristics of a dual fuel engine operated on alternative gaseous fuels. Fuel 2013;109:669–78. http://dx.doi.org/10.1016/j.fuel.2013.03.007.
[20] Diéguez PM, Urroz JC, Marcelino-Sádaba S, Pérez-Ezcurdia A, Benito-Amurrio M, Sáinz D, et al. Experimental study of the performance and emission characteristics of an adapted commercial four-cylinder spark ignition engine running on hydrogen–methane mixtures. Appl Energy 2014;113:1068–76. http://dx.doi.org/10.1016/j.apenergy.2013.08.063.
[21] Yang L, Ge X, Wan C, Yu F, Li Y. Progress and perspectives in converting biogas to transportation fuels. Renew Sustain Energy Rev 2014;40:1133–52. http://dx.doi.org/10.1016/j.rser.2014.08.008.
[22] Rakopoulos DC, Rakopoulos CD, Giakoumis EG. Impact of properties of vegetable oil, bio-diesel, ethanol and n-butanol on the combustion and emissions of turbocharged HDDI diesel engine operating under steady and transient conditions. Fuel 2015;156:1–19. http://dx.doi.org/10.1016/j.fuel.2015.04.021.
[23] Millo F, Debnath BK, Vlachos T, Ciaravino C, Postrioti L, Buitoni G. Effects of different biofuels blends on performance and emissions of an automotive diesel engine. Fuel 2015;159:614–27. http://dx.doi.org/10.1016/j.fuel.2015.06.096.
[24] Rajesh Kumar B, Saravanan S, Rana D, Nagendran A. Use of some advanced biofuels for overcoming smoke/NO_x trade-off in a light-duty DI diesel engine. Renew Energy 2016;96:687–99. http://dx.doi.org/10.1016/j.renene.2016.05.029.
[25] Henham A, Makkar M. Combustion of simulated biogas in a dual-fuel diesel engine. Energy Convers Manag 1998;39:2001–9. http://dx.doi.org/10.1016/S0196-8904(98)00071-5.
[26] Karim G. Hydrogen as a spark ignition engine fuel. Int J Hydrogen Energy 2003;56:256–63.
[27] Talibi M, Hellier P, Balachandran R, Ladommatos N. Effect of hydrogen-diesel fuel co-combustion on exhaust emissions with verification using an in–cylinder gas sampling technique. Int J Hydrogen Energy 2014;39:15088–102. http://dx.doi.org/10.1016/j.ijhydene.2014.07.039.
[28] Lilik G, Zhang H, Herreros J. Hydrogen assisted diesel combustion. Int J Hydrogen Energy 2010;35:4382–98. http://dx.doi.org/10.1016/j.ijhydene.2010.01.105.
[29] Tsolakis A, Hernandez J. Dual fuel diesel engine operation using H2. Effect on particulate emissions. Energy & Fuels 2005:418–25.
[30] Masood M, Ishrat M, Reddy A. Computational combustion and emission analysis of hydrogen–diesel blends with experimental verification. Int J Hydrogen Energy 2007;32:2539–47. http://dx.doi.org/10.1016/j.ijhydene.2006.11.008.
[31] Saravanan N, Nagarajan G, Kalaiselvan KM, Dhanasekaran C. An experimental investigation on hydrogen as a dual fuel for diesel engine system with exhaust gas recirculation technique. Renew Energy 2008;33:422–7. http://dx.doi.org/10.1016/j.renene.2007.03.015.
[32] Ladommatos N, Balian R, Horrocks R, Cooper L. The effect of exhaust gas recirculation on soot formation in a high-speed direct-injection diesel engine. SAE Paper. 1996. p. 960841. http://dx.doi.org/10.4271/960841.
[33] Ladommatos N, Abdelhalim S, Zhao H. The effects of exhaust gas recirculation on diesel combustion and emissions. Int J Engine Res 2000;1:107–26. http://dx.doi.org/10.1243/1468087001545290.
[34] Bose PK, Maji D. An experimental investigation on engine performance and emissions of a single cylinder diesel engine using hydrogen as inducted fuel and diesel as injected fuel with exhaust gas recirculation. Int J Hydrogen Energy 2009;34:4847–54. http://dx.doi.org/10.1016/j.ijhydene.2008.10.077.
[35] Miyamoto T, Hasegawa H, Mikami M, Kojima N, Kabashima H, Urata Y. Effect of hydrogen addition to intake gas on combustion and exhaust emission characteristics of a diesel engine. Int J Hydrogen Energy 2011;36:13138–49. http://dx.doi.org/10.1016/j.ijhydene.2011.06.144.
[36] Shin B, Cho Y, Han D, Song S, Chun KM. Hydrogen effects on NOx emissions and brake thermal efficiency in a diesel engine under low-temperature and heavy-EGR conditions. Int J Hydrogen Energy 2011;36:6281–91. http://dx.doi.org/10.1016/j.ijhydene.2011.02.059.
[37] Banerjee R, Roy S, Bose PK. Hydrogen-EGR synergy as a promising pathway to meet the PM–NOx–BSFC trade-off contingencies of the diesel engine: a comprehensive review. Int J Hydrogen Energy 2015;40:12824–47. http://dx.doi.org/10.1016/j.ijhydene.2015.07.098.
[38] Heywood JB. Internal combustion engine fundamentals. 1st ed. New York: McGraw-Hill; 1988.
[39] Stone R. Introduction to internal combustion engines. 4th ed. New York: Palgrave Macmillan Limited; 2012.
[40] Verhelst S, Maesschalck P, Rombaut N, Sierens R. Increasing the power output of hydrogen internal combustion engines by means of supercharging and exhaust gas recirculation. Int J Hydrogen Energy 2009;34:4406–12. http://dx.doi.org/10.1016/j.ijhydene.2009.03.037.
[41] Nagalingam B, Dübel M, Schmillen K. Performance of the supercharged spark ignition hydrogen engine. 1983. http://dx.doi.org/10.4271/831688.
[42] Furuhama S, Fukuma T. High output power hydrogen engine with high pressure fuel injection, hot surface ignition and turbocharging. Int J Hydrogen Energy 1986;11:399–407. http://dx.doi.org/10.1016/0360-3199(86)90029-7.
[43] Lynch F. Parallel induction: a simple fuel control method for hydrogen engines. Int J Hydrogen Energy 1983;8:721–30. http://dx.doi.org/10.1016/0360-3199(83)90182-9.

[44] Roy MM, Tomita E, Kawahara N, Harada Y, Sakane A. An experimental investigation on engine performance and emissions of a supercharged H2-diesel dual-fuel engine. Int J Hydrogen Energy 2010;35:844–53. http://dx.doi.org/10.1016/j.ijhydene.2009.11.009.
[45] Gunea C, Razavi MRM, Karim GA. The effects of pilot fuel quality on dual fuel engine ignition delay. SAE Paper. 1998. p. 982453. http://dx.doi.org/10.4271/982453.
[46] Prakash G, Ramesh A, Shaik AB. An approach for estimation of ignition delay in a dual fuel engine. 1999. http://dx.doi.org/10.4271/1999-01-0232.
[47] Kittelson D, Watts W, Johnson J. Diesel aerosol sampling methodology – CRC E-43. Minneapolis, USA. 2002.
[48] Raaschou-Nielsen O, Andersen ZJ, Beelen R, Samoli E, Stafoggia M, Weinmayr G, et al. Air pollution and lung cancer incidence in 17 European cohorts: prospective analyses from the European study of cohorts for air pollution effects (ESCAPE). Lancet Oncol 2013;14:813–22. http://dx.doi.org/10.1016/S1470-2045(13)70279-1.